Reduced Expression of Cerebral Metabotropic Glutamate Receptor Subtype 5 in Men with Fragile X Syndrome

James R. Brašić [1],*, **Ayon Nandi [1]**, **David S. Russell [2,3]**, **Danna Jennings [2,3,4]**,
Olivier Barret [2], **Anil Mathur [1]**, **Keith Slifer [5,6]**, **Thomas Sedlak [1,7]**, **Samuel D. Martin [1,8]**,
Zabecca Brinson [1], **Pankhuri Vyas [1]**, **John P. Seibyl [2,3]**, **Elizabeth M. Berry-Kravis [9]**,
Dean F. Wong [1,10] and **Dejan B. Budimirovic [5,11],***

[1] Section of High Resolution Brain Positron Emission Tomography Imaging, Division of Nuclear Medicine and Molecular Imaging, The Russell H. Morgan Department of Radiology and Radiological Science, The Johns Hopkins University School of Medicine, Baltimore, MD 21287, USA; anandi1@jhmi.edu (A.N.); amathur4@jhmi.edu (A.M.); tsedlak@jhmi.edu (T.S.); smart149@jhu.edu (S.D.M.); zabecca.brinson@gmail.com (Z.B.); pankhuri.v@gmail.com (P.V.); dfwong@wustl.edu (D.F.W.)

[2] Clinical Research, Institute for Neurodegenerative Disorders, New Haven, CT 06510, USA; drussell@invicro.com (D.S.R.); Jennings@dnli.com (D.J.); olivier.barret@cea.fr (O.B.); jseibyl@invicro.com (J.P.S.)

[3] Research Clinic, Invicro LLC, New Haven, CT 06510, USA

[4] Denali Therapeutics, Inc., South San Francisco, CA 94080, USA

[5] Department of Psychiatry and Behavioral Sciences-Child Psychiatry, The Johns Hopkins University School of Medicine, Baltimore, MD 21205, USA; slifer@kennedykrieger.org

[6] Department of Behavioral Psychology, Kennedy Krieger Institute, Baltimore, MD 21205, USA

[7] Department of Psychiatry and Behavioral Sciences-General Psychiatry, The Johns Hopkins University School of Medicine, Baltimore, MD 21205, USA

[8] Department of Neuroscience, Zanvyl Krieger School of Arts and Sciences, The Johns Hopkins University, Baltimore, MD 21218, USA

[9] Departments of Pediatrics, Neurological Sciences, and Biochemistry, Rush University Medical Center, Chicago, IL 60612, USA; Elizabeth_Berry-Kravis@rush.edu

[10] Precision Radio-Theranostics Translational Laboratories, Mallinckrodt Institute of Radiology, School of Medicine, Washington University, Saint Louis, MO 63110, USA

[11] Departments of Psychiatry and Neurogenetics, Kennedy Krieger Institute, Baltimore, MD 21205, USA

* Correspondence: jbrasic1@jh.edu (J.R.B.); budimirovic@kennedykrieger.org (D.B.B.); Tel.: +1-410-986-0341 (J.R.B.); +1-443-923-2634 (D.B.B.)

Abstract: Glutamatergic receptor expression is mostly unknown in adults with fragile X syndrome (FXS). Favorable behavioral effects of negative allosteric modulators (NAMs) of the metabotropic glutamate receptor subtype 5 (mGluR$_5$) in *fmr1* knockout (KO) mouse models have not been confirmed in humans with FXS. Measurement of cerebral mGluR$_5$ expression in humans with FXS exposed to NAMs might help in that effort. We used positron emission tomography (PET) to measure the mGluR$_5$ density as a proxy of mGluR$_5$ expression in cortical and subcortical brain regions to confirm target engagement of NAMs for mGluR$_5$s. The density and the distribution of mGluR$_5$ were measured in two independent samples of men with FXS ($N = 9$) and typical development (TD) ($N = 8$). We showed the feasibility of this complex study including MRI and PET, meaning that this challenging protocol can be accomplished in men with FXS with an adequate preparation. Analysis of variance of estimated mGluR$_5$ expression showed that mGluR$_5$ expression was significantly reduced in cortical and subcortical regions of men with FXS in contrast to age-matched men with TD.

1. Introduction

1.1. Background

Fragile X syndrome (FXS) is caused by expansion full mutation (≥200 CGGs) of the fragile X mental retardation 1 *(FMR1)* gene leading to epigenetic silencing of the gene, resulting in reduction of its product: fragile X mental retardation protein (FMRP) [1]. FXS is the leading single-gene cause of inherited intellectual disability (ID) and autism spectrum disorder (ASD) [2,3]. Indeed, studies of humans with FXS have consistently demonstrated a wide range of global neurobehavioral impairments [4–9]. This is not surprising, as FMRP controls translation around 4% of mRNA in human brains. To illustrate, FMRP binds brain mRNAs, inhibits synthesis of a myriad of proteins [10], and increases the dosages of FMRP target proteins (over 600 to date) of relevance to ASD [11]. The FMRP expression in the brain is the ultimate factor determining the severity of the neurobehavioral phenotype [12]. The absence of adequate FMRP results in overactive glutamatergic signaling of group 1 metabotropic (mGluR$_1$ and mGluR$_5$) pathways, and consequently overactive downstream signaling cascades, such as the mammalian target of rapamycin (mTOR) and mitogen-activated protein kinase (MAPK)/extracellular signal-regulated kinase (ERK). The overactive downstream signaling leads to excessive protein synthesis in an *fmr1* knockout (KO) mouse model [13]. Namely, abnormal mGluR$_5$-modulated long-term depression (LTD) in the hippocampus in the *fmr1* KO model led to "the mGluR$_5$ theory" of neuronal dysfunction in FXS [14]. Indeed, the abnormal signaling in the absence of FMRP is associated with aberrant synaptic plasticity and immature dendritic spine morphology. The abnormal excitation–inhibition that leads to an excessive de novo protein synthesis also occurs in humans with FXS [15–18]. Targeted treatment studies using mGluR$_5$ negative allosteric modulators (NAMs) then unfolded in both the *fmr1* KO mouse model and in humans with FXS [3,12]. Yet, mGluR$_5$ expression in animal studies and in autopsy studies of humans with FXS produced inconsistent results. Moreover, mGluR$_5$ expression in vivo has not been measured in humans with FXS.

Although a necropsy study pooling human brains with FXS and premutation of the *FMR1* gene (PM, 55–200 CGGs) showed increased mGluR$_5$s and marginal protein overexpression [19], these studies do not exist in the living human brain. Since the limited necropsy findings may represent the changes in agonal and post-mortem periods, in vivo measurement of the expression of mGluR$_5$s is needed, which may bring an initial insight into failed clinical trials that used investigational agents acting on mGluR$_5$ in humans FXS. Novel, specific mGluR$_5$ ligands that allow quantitative measurement of the density and distribution of mGluR$_5$s in the brain, such as 3-[^{18}F]fluoro-5-(2-pyridinylethynyl)benzonitrile ([^{18}F]FPEB), require studies of feasibility.

Indeed, quantification of mGluR$_5$ expression in the living human brain of men with FXS is needed to help understand results of past mGluR$_5$ trials in humans with FXS, and to help provide information for successful clinical trial designs. For example, an alteration of expression of mGluR$_5$s, such as internalization of membrane mGluR$_5$s, may be one possible explanation for the negligible therapeutic effect of NAMs in "failed" clinical trials of humans with FXS [20]. Since proteins and receptors occupy different locations on the membranes, the living brain may show protein overexpression and reduction of receptors due to receptor internalization or other alterations. Thus, the use of [^{18}F]FPEB may serve as an effective tool to confirm target engagement of NAMs for mGluR$_5$s.

1.2. Measurement of mGluR$_5$s in the Living Human Brain

While several techniques exist to estimate the concentration of glutamate in the living brain, including magnetic resonance imaging (MRI) and brain biopsy, positron emission tomography (PET) uniquely provides the optimal means to measure mGluR$_5$s. For these reasons, radiotracers that bind to mGluR$_5$ in the living brain and can be visualized with PET are promising tools to quantify the density and the distribution of mGluR$_5$s in humans with FXS.

[^{18}F]FPEB

3-[^{18}F]fluoro-5-(2-pyridinylethynyl)benzonitrile ([^{18}F]FPEB), a novel, specific mGluR$_5$ ligand to quantitatively measure the density and distribution of mGluR$_5$s in the brain regions of humans with FXS through PET [21–30] (Figure 1), constitutes an effective tool to confirm target engagement of mGluR$_5$s of relevance to clinical trials of NAMs for individuals with FXS [31].
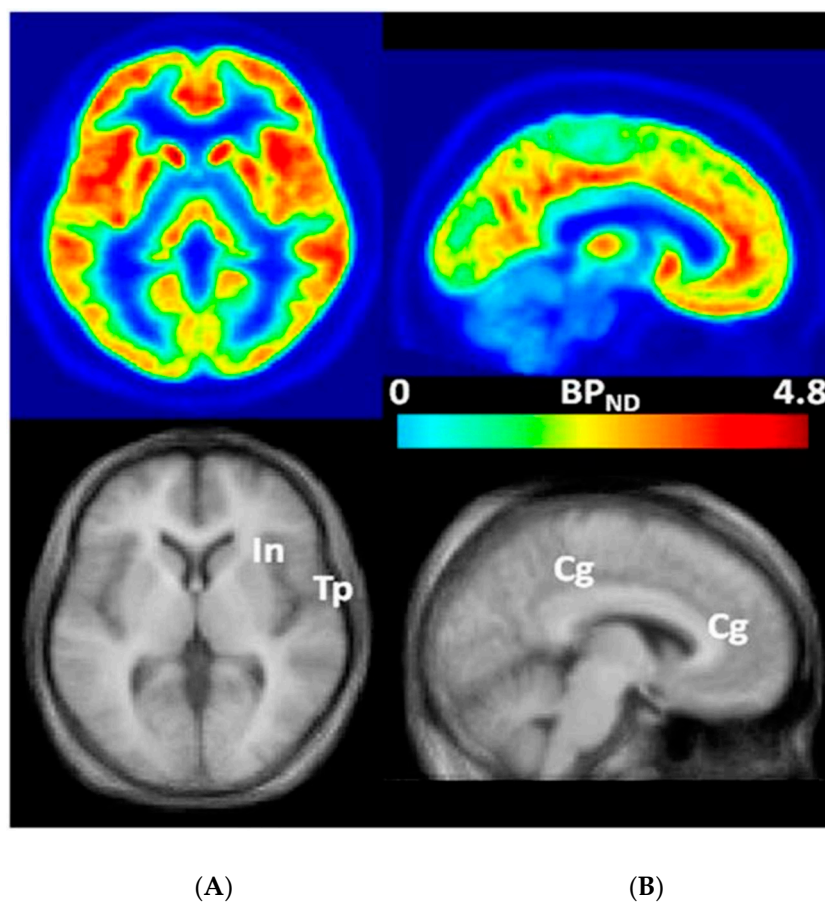

(**A**)   (**B**)

Figure 1. Transaxial (**A**) and sagittal (**B**) non-displaceable binding potential (BP$_{ND}$) [32] images of [^{18}F]FPEB (**top**) and matching magnetic resonance (MR) images (**bottom**) in statistical parametric mapping (SPM) [33] standard space. Regions with high BP$_{ND}$ values, namely insular (In), temporal (Tp), and cingulate (Cg) cortices, are indicated on co-registered MR images [30]. This research was originally published in *JNM*. Wong DF, Waterhouse R, Kuwabara H, Kim J, Brašić JR, Chamroonrat W, Stabins M, Holt DP, Dannals RF, Hamill TG, Mozley PD. ^{18}F-FPEB, a PET radiopharmaceutical for quantifying metabotropic glutamate 5 receptors: a first-in-human study of radiochemical safety, biokinetics, and radiation dosimetry. J Nucl Med. 2013;54:388-396. © SNMMI [30].

Specifically, [^{18}F]FPEB [22,34–37] has been shown to demonstrate high uptake and specific binding during the test–retest paradigm for mGluR$_5$ in the anterior cingulate gyrus, putamen, caudate nucleus, and frontal, parietal, and temporal cortices [28,29]. [^{18}F]FPEB has demonstrated deficits in the striatal

and neocortical mGluR$_5$s in people with mild Huntington's disease [34,35] and increments in the mGluR$_5$s in people with mild Parkinson's disease [36–38] and men with ASD [25].

We sought to quantify the density and distribution of mGluR$_5$ expression in FXS [39–51] by means of PET.

2. Materials and Methods

2.1. Participants

2.1.1. Recruiting Sites

The study is approved by Johns Hopkins Medicine Institutional Review Board IRB 169 249. The protocols for the study of humans with FXS were approved by the Institutional Review Boards of the Institute for Neurodegenerative Disorders (IND) in New Haven, Connecticut [52] and Johns Hopkins University (JHU) in Baltimore, Maryland [53,54]. Since exposure to radioactivity in PET constitutes greater than minimal risk, this pilot study was restricted to adults. Written informed consent was obtained from each participant at both locations.

2.1.2. Inclusion Criteria

Inclusion criteria for all subjects were age 18–60 years and a diagnosis of FXS based on *FMR1* DNA gene testing by PCR/Southern Blot, supplemented by clinical neurobehavioral profiling [52].

2.1.3. Exclusion Criteria

Exclusion criteria were clinically significant abnormal laboratory values and/or clinically significant unstable serious medical, neurological, or psychiatric illnesses [52].

2.1.4. Institute for Neurodegenerative Disorders (IND)

Participants with FXS had completed genetic and other evaluations before traveling to the IND with a caregiver. One day after arrival to the IND, they underwent a screening assessment to confirm the inclusion and exclusion criteria, neuropsychological evaluation, mock scanner training, and PET scans. Participants with TD were recruited from community residents.

Seven men with FXS (mean age 25 ± 5, range 23–34 years) recruited from Rush University Medical Center, Chicago, Illinois, and three age-matched men with typical development (TD) (mean aged 32 ± 4, range 27–39 years) participated in the protocol. Clinical and demographic data [55] confirmed that all participants met the criteria to receive the adult dose of 185 megabecquerels (MBqs) (5 millicuries (mCis)) of [^{18}F]FPEB.

2.1.5. Johns Hopkins University (JHU)

Four men with FXS (mean age 28 ± 9, range 19–41 years) were recruited from the Kennedy Krieger Institute, Baltimore, Maryland, and Rush University Medical Center, including referrals from the Fragile X Online Registry With Accessible Research Database (FORWARD) of the National Fragile X Foundation (NFXF) funded by the Centers for Disease Control and Prevention (CDC), Atlanta, Georgia. The results of two of the four men with FXS (mean age 25.5 ± 2.1, range 24–27) who completed PET scans were reported in this article. Findings were compared and contrasted with five age-matched historical control men with TD who had already completed similar protocols (mean age 29.6 ± 6.02, range 24–39 years) [25,30]. Clinical and demographic data confirmed that all participants met the criteria to receive the adult dose of 185 MBqs (5 mCis) of [^{18}F]FPEB [55].

2.2. Assessments

2.2.1. Institute for Neurodegenerative Disorders (IND)

Assessments of participants with FXS (600 to 1600 CGGs) included mean FMRP of 0.047 ± 0.04 ng/microgram total protein (reference mean FMRP of 0.87 for healthy normal controls with TD), reading level under first grade level, and scores for the Dementia Screening Questionnaire for Individuals with Intellectual Disabilities (DSQIID) [56] ranging from 0 to 2 [55].

2.2.2. Johns Hopkins University (JHU)

Assessments of participants with FXS (>200 CGGs) included mean FMRP of 0.00025, mean abbreviated IQ [57,58] of 48.5 ± 2.12 [55], and mean Adaptive Behavior Composite Standard Score [59] of 71.5 ± 26.16 [55].

2.3. Procedures

2.3.1. Magnetic Resonance Imaging (MRI)

IND

In order to minimize anxiety and claustrophobia, participants with FXS at the IND did not undergo MRI. Participants with TD underwent MRI to compare and contrast with other cohorts (N = 3) [52,55].

JHU

Participants with FXS and TD at JHU underwent MRI (Table 1) to rule out intracranial pathology and to co-register with PET [55].

Table 1. Characterization of MRI sequences of the brain.

Format	Time to Repetition (TR) (ms)	Time to Echo (TE) (ms)	Thickness (mm)	Number of Slices
T1 sagittal	500	8	5.0	21
T1 SPGR recalled acquisition in the steady-state axial	35	6	1.5	124
T2 oblique	5900	95	5.0	27
DTI	12,100	88	2.0	72

Reproduced with permission [60]. The parameters of DTI include a slice thickness of 2 × 2 × 2 mm, field of view of 240 mm, iPAT (acceleration factor) of 2, 30 directions, and a b value of 1000 s/mm^2. Abbreviations: MRI, magnetic resonance imaging; DTI, diffusion tensor imaging; SPGR, spoiled gradient.

2.3.2. Positron Emission Tomography (PET)

IND

With the head stabilized by a gauze strip taped across the forehead and a rounded head holder, each participant received an intravenous bolus injection of 185 MBqs (5 mCis) of [18F]FPEB [30] at 1 PM, followed by scans on an ECAT EXACT HR+ PET attaining an axial resolution of approaching y = 4–5 mm [61], with consecutive 6 × 300 s frames performed for 90 to 120 min after the injection time.

Statistical parametric mapping (SPM) [33] was applied to PET frames to obtain regional time (radioactivity) curves (TACs). The ratio of uptake in the volumes of interest (VOIs) to the uptake in the whole cerebellum, a reference region with minimal [18F]FPEB uptake [28,29], was calculated.

JHU

MRI was performed an hour before PET. Each participant with FXS underwent training using a mock scanner [62–64]. Each participant had a custom fitted face mask made by nuclear medical technologists to hold the head in the same position throughout the scan [65,66]. After receiving

intravenous bolus injections of 185 MBq (5 mCis) of [^{18}F]FPEB (30), participants underwent PET scans on a high resolution research tomograph (HRRT), attaining an axial resolution approaching 2.3 to 2.5 mm [67,68] at 1 PM for 90 min.

VOIs were obtained automatically of cortical regions with Freesurfer 6.0 [69,70] and of subcortical regions with the subcortical segmentation tools of the software library of the Oxford Centre for fMRI of the Brain [71–73]. VOIs were transferred from MRI to PET space according to MRI-to-PET co-registration parameters obtained with the co-registration module [74,75] of statistical parametric mapping (SPM) [33] and applied to PET frames to obtain regional TACs. With the cerebellar white matter as the reference VOI [28,29], regional BP$_{ND}$s [32] were obtained by reference tissue graphical analysis (RTGA) [76,77].

2.3.3. Comparisons and Contrasts of Cohorts from the IND and JHU

In order to directly compare and contrast data from both cohorts including nine men with FXS (mean age 27.21 ± 4.17, range 22.3–33.6) and eight historical control age-matched men with TD who had already completed similar protocols (mean age 30.63 ± 5.58, range 24–39 years) [25,30,52,55], we approximated the data with several estimates by means of multiple assumptions: (1) consistency over time of both standard uptake volume ratios (SUVRs) and distribution volume ratios (DVRs), since JHU PET scans spanned 0 to 90 min after radiotracer injections, while IND PET scans spanned 90–120 min; (2) approximately equivalent anatomical brain regions, as MRI-based segmentation was utilized for VOI analysis at JHU, but an atlas-based approach was applied to the IND data; and (3) approximately equivalent analyses, although the resolution of the scans from the IND was approximately twice the resolution of scans from JHU. Using the measurements of SUVR from the IND dataset, we derived estimates of binding potentials as DVR-1 [78], which were pooled with the comparable BP$_{ND}$ estimates from the JHU data.

3. Results

3.1. mGluR$_5$s in Humans with FXS

3.1.1. IND

The density of mGluR5s was comparable in the men with FXS and the men with TD (Figure 2) [55].
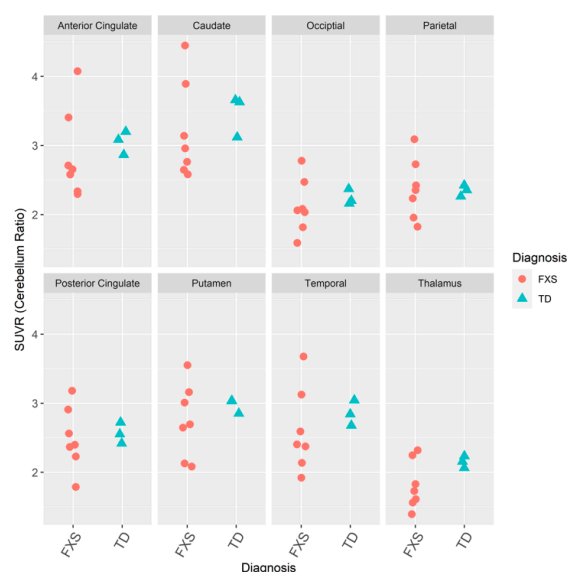

Figure 2. Dot plots of the ratio of densities of mGluR$_5$ in volumes of interest (VOIs) to whole cerebellum for participants from the Institute for Neurodegenerative Disorders (IND) with FXS (*N* = 7) and TD (*N* = 3) who received intravenous bolus injections of 185 MBqs (5 mCis) of [^{18}F]FPEB [55,79].

3.1.2. JHU

Participant JHUFXS1 withdrew before scans due to a family emergency.

Participant JHUFXS2 completed both MRI and PET scans in one day without mock scanner training.

Due to scheduling problems, MRI and PET scans were conducted on Participant JHUFXS3 on separate days a week apart without mock scanner training. Despite the administration of 2.0 mg of lorazepam before each scan, he could not complete either scan due to anxiety and agitation.

Participant JHUFXS4 had already completed MRI scans of 30 and 60 min on separate days at another institution. For this prior investigation, a psychologist met with him online regularly for weeks before the scans to practice holding still despite the noise. He had never had a PET scan. His mother began practicing relaxation and holding still while listening to MRI sounds for weeks before the session at JHU. His mother and an investigator accompanied him into the MRI chamber throughout the MRI scan. His mother sat at the operator's booth throughout the PET scan to praise him for holding still during the PET scan.

The non-displaceable binding potentials (BP_{ND}s) [32] of [18F]FPEB by reference tissue graphical analysis (RTGA) [76,77] in each VOI of two men with FXS were below the BP_{ND}s of five age-matched men with TD [25,30,55] (Figure 3). $mGluR_5$ expression was lower in the men with FXS than the men with TD (Figure 3).
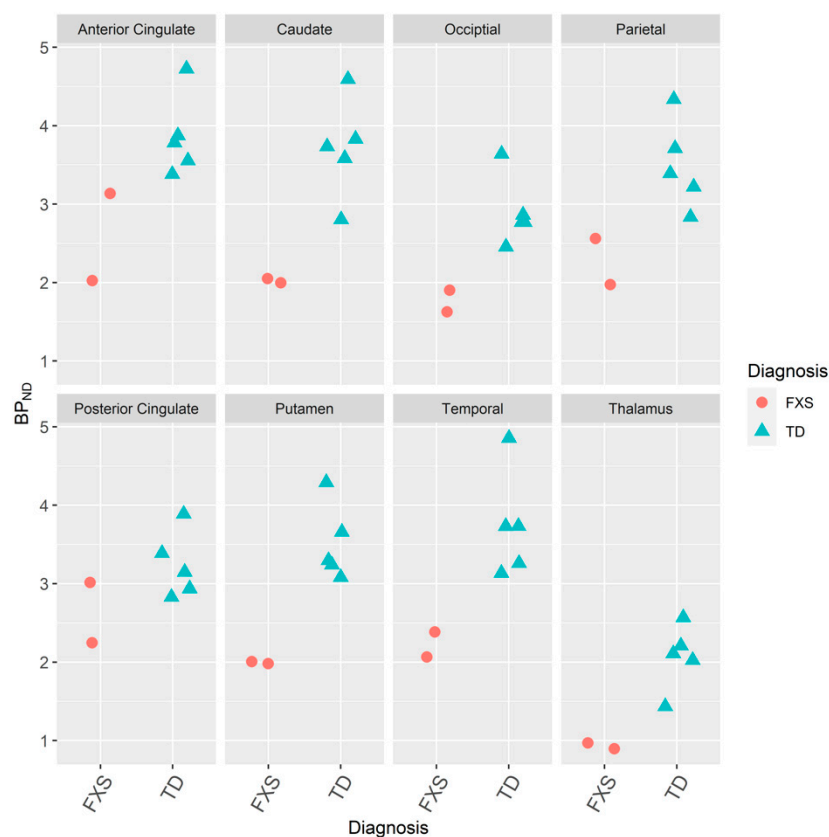

Figure 3. Dot plot of non-displaceable binding potential (BP_{ND}) [32] images by reference tissue graphical analysis (RTGA) [76,77] of volumes of interest on positron emission tomography (PET) for 90 min of participants with FXS and ID (*N* = 2) and TD (*N* = 5) who received intravenous bolus injections of 185 MBqs (5 mCis) of [18F]FPEB [25,30,55,79].

3.1.3. IND and JHU

Combined (IND and JHU) estimates of $mGluR_5$ were significantly reduced in all eight volumes of interest (anterior cingulate, caudate, occipital, parietal, posterior cingulate, putamen, temporal, and thalamus) in the men with FXS (*N* = 9) in contrast to the age-matched men with TD (Figure 4, Table 2).

Although the axial resolution of the IND scans was approximately twice that of the JHU scans, the combined results are striking.
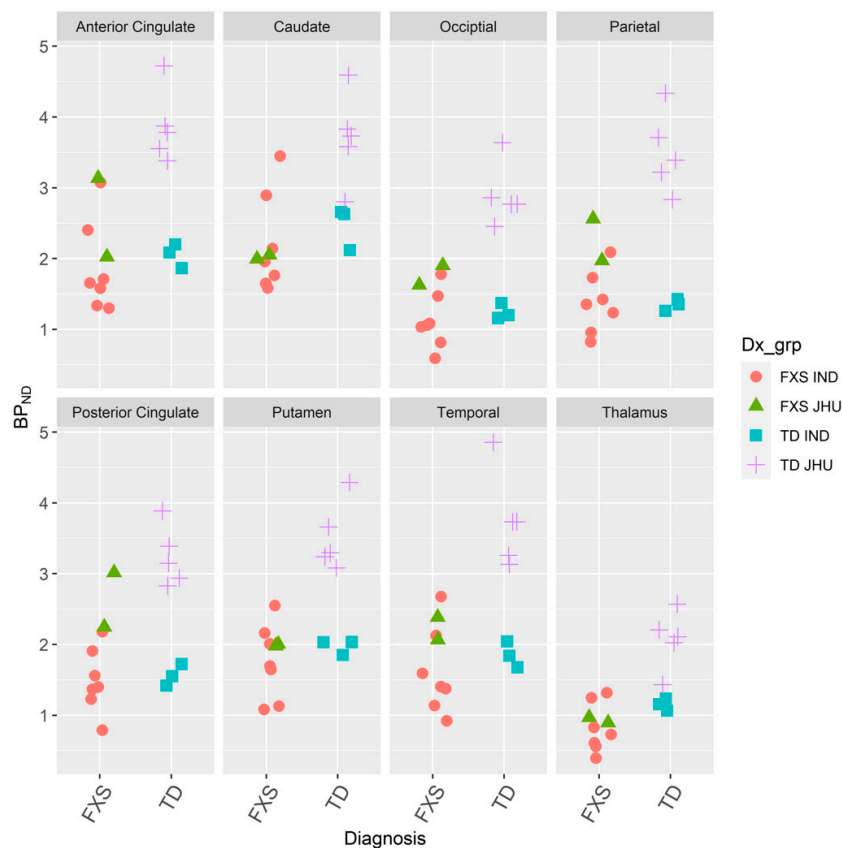

Figure 4. Dot plot of estimated binding potential (BP) [32] images by positron emission tomography after intravenous bolus injections of 185 MBqs (5 mCis) of [^{18}F]FPEB [25,30] for men with fragile X syndrome (*N* = 9) and age-matched men with typical development (*N* = 8) from the IND and JHU [52,55,79].

Table 2. Analysis of variance of estimates of mGluR$_5$ expression by positron emission tomography after intravenous bolus injections of 185 MBqs (5 mCis) of [^{18}F]FPEB in cortical and subcortical regions in the combined sample of men with fragile X syndrome (*N* = 9) and age-matched men with typical development (*N* = 8).

Region	Term	*df*	Sum of Squares	F Statistic	*p*-Value
Anterior Cingulate	Diagnosis	1	5.69	15.1	0.00165
	Source	1	5.93	15.7	0.00141
Caudate	Diagnosis	1	4.93	10.6	0.00569
	Source	1	1.22	2.62	0.128
Occipital	Diagnosis	1	4.37	23.1	0.000279
	Source	1	4.92	26	0.000163
Parietal	Diagnosis	1	5.32	18.9	0.000675
	Source	1	8.58	30.4	0.000076
Posterior Cingulate	Diagnosis	1	3.18	17.6	0.000906
	Source	1	7.04	38.9	2.18E-05
Putamen	Diagnosis	1	5.4	18.4	0.000753
	Source	1	3.1	10.6	0.00583
Temporal	Diagnosis	1	7.07	17.9	0.000834
	Source	1	5.92	15	0.00169
Thalamus	Diagnosis	1	3.32	23.7	0.000249
	Source	1	1.06	7.55	0.0157

Furthermore, a two-way analysis of variance on an initial pooled dataset showed that both independent variables of institution (IND and JHU, *df* = 1, F = 34.3, *p* < 0.0001) as well as diagnosis (FXS and TD, *df* = 1, F = 38.7, *p* < 0.0001) had non-random effects on regional estimates of BP [80] (Table 2).

4. Discussion

We showed the feasibility and safety of administering MRI and PET in two independent pilot samples of men with FXS. We applied PET to quantitatively measure the density of mGluR$_5$s in cortical and subcortical brain regions of these men with FXS following exposure to [^{18}F]FPEB), which is a first study to our knowledge. We found that mGluR$_5$ density was significantly reduced in the cingulate, cortex, striatum, and thalamus in men with FXS in contrast to age-matched men with TD. The tracer is a novel, specific mGluR$_5$ ligand to measure the density and distribution of mGluR$_5$s in the brains of humans, which constitutes an effective tool to confirm target engagement of NAMs for mGluR$_5$s. The feasibility of this complex protocol requires a multidisciplinary effort that includes mock scanner training and practice sessions taught with behavioral psychology.

4.1. mGluR$_5$s in Humans with FXS

4.1.1. Feasibility of a Complex Protocol of MRI and PET Scans in Participants with FXS

Adults

A primary goal of this study was to determine the feasibility and safety of a complex protocol that included MRI and PET scans on men with FXS. We showed that this challenging protocol can be accomplished with mock scanner training and practice sessions taught with behavioral psychology [62–64] and trained parents. Additionally, an investigator and a parent routinely accompanied participants into the MRI chamber to assist with the process during the entire MRI series. Since state-of-the-art PET scanners provide three-dimensional image reconstruction, face masks may no longer be required to stabilize heads. Scans may be accomplished with gauze for optimal comfort.

We recommend several modifications to facilitate the completion of the MRI and PET scans on individuals with FXS. Mock scanner training beginning online for weeks before the actual scans provides the means to train participants and parents to relax quietly without moving while loud noises like a jackhammer are played [62–64]. Behavioral psychologists can meet with participants and parents repeatedly online to utilize training sessions for holding still while MRI soundtracks are played through recordings. The sessions can begin with short practices of 15 s. Gradually, the duration of the session can be increased to 30 or 60 min to train participants to calmly endure the challenges of the noise and stillness. Additionally, behavioral psychologists can provide the example of providing positive feedback to the participants. In other words, praising the participant for holding still during the practice session is a valuable positive reinforcement for desired behavior. On the other hand, criticizing the participant for moving may increase anxiety and lead to agitation and uncooperative behavior. Therefore, parents can be taught to reward the desired behavior.

Another approach to facilitate successful completion of scans includes the shortening of the duration of PET scans and the use of gauze instead of a rigid face mask. Additionally, performing PET and MRI scans on two separate days allows participants to recover from the stress of one scan before undergoing the next. The use of PET/MRI machines would simplify the protocol to accomplish both PET and MRI in a single session [81].

Adolescents and Children

Since PET involves greater than minimal risk due to radiation exposure, the safety and efficacy must be shown in adults before exposing vulnerable populations. For this reason, the current protocol was administered only to adults with FXS. After safety and efficacy are established in adults, then

the procedure will be sequentially administered to adolescents, followed by children. The procedure may be modified for children to reduce the duration of scans. The procedure of the IND to conduct a 30 min scan 90 to 120 min after radiotracer injection with gauze to stabilize the head will shorten the stress of remaining on the scanner table. Another modification will be the utilization of PET/MRI scanners to conduct both PET and MRI scans in a single session instead of separate sessions for PET and MRI scans [81]. Mock scanner training by experienced behavioral psychologists [62–64] will be crucial to prepare children and adolescents for scans. Additionally, the participation of parents for each step is key to the accomplishment of this challenging protocol.

4.2. mGluR$_5$ Measurement in Men with FXS

Another goal of this investigation was to find out if the study protocol can quantify mGluR$_5$ expression in the brains of adult males with FXS. The data from our study show that the PET ligand binds mGluR$_5$s in the brains of men with FXS, and that the expression of these receptors is decreased. This finding could be mediated by excessive upstream signaling resulting in reduced expression of mGluR$_5$s. Internalization of the mGluR$_5$s [20,82] throughout the brain induced by the radiotracer, the scanner, or other aspects of the environment of PET scans may explain the reductions in mGluR$_5$s in our participants with FXS.

A preliminary attempt to perform an analysis on a combined dataset of both FXS/TD data from the IND and JHU showed that the source of the data was a non-random factor that influenced the outcome variable. We shall strive to reduce this possible confounding influence to improve the effect size in future analyses. As a future direction, we are developing other means of analyzing larger datasets from multiple institutions in a comparable manner so that the data can be pooled after removing the confounding factors of methodological differences.

4.3. Avoiding Effects of Diurnal Variations of mGluR$_5$s

We administered PET scans to participants with FXS at the same time of day (1 PM) to minimize effects of diurnal variations of mGluR$_5$s. Participants with TD received radiotracer injections 32 ± 120 min (range -135 to $+163$) from 1 PM [55], resulting in a confounding influence of diurnal variation. Large alterations in radiotracer uptake on the same individuals during the same day suggest that there may be considerable diurnal variation in mGluR$_5$s, with increased uptake later in the day [21,83–85]. Participants with FXS may experience greater anxiety with scans than participants with TD. Anxiety may increase cortisol values and result in diurnal variations. Thus, we assume that our participants with FXS likely exhibited the maximal radiotracer uptake at the time of their scans. Measurement of cortisol levels and administration of PET scans at the same time of day to all participants minimizes the effects diurnal variations of mGluR$_5$s.

4.4. Limitations and Future Studies

There is a need for comprehensive protocols uniformly administered to all cohorts. The use of different protocols for PET at the collaborating institutions [52,86] confounds comparisons and contrasts of the results. Future investigations at multiple centers will benefit from the use of identical protocols and analyses for PET and MRI conducted contemporaneously. Analysis of results by a single center will facilitate the uniformity of the findings. Despite different protocols, the uniformity of the finding of reduced mGluR$_5$ expression in multiple brain regions independent of protocol strengthens this study's key finding.

Administration of the full neuropsychological battery to contemporaneous cohorts at all participating centers will provide the foundation to apply statistical analyses. Normalization of cognitive test scores for participants with FXS will remove a "floor effect" [58]. Future studies will benefit from examining participants with FXS exhibiting a spectrum of ID and ASD and comparison groups without FXS with levels of ID matched to the participants with FXS.

The current pilot study is limited by the incomplete *FMR1* gene and epigenetic (methylation) parameter identification, and incomplete size mosaicism and quantification of FMRP. Future studies will be enhanced by including these measures and whole exome sequencing (WES) [87] on all participants to test the hypothesis that the parameters are correlated [12].

Since increased protein synthesis has been demonstrated in fibroblasts of individuals with FXS and *fmr1* KO mice [88], measurement of protein synthesis, particularly in the mTOR and ERK signaling cascades, would be a valuable parameter to correlate with mGluR$_5$ density and distribution in future investigations of FXS in humans. However, the absence of increased protein synthesis in young men with FXS sedated with dexmedetomidine for PET with L[1-^{11}C]leucine suggests that humans with FXS may not demonstrate the increased protein synthesis seen in animal models [89].

Multimodal Imaging

Multimodal imaging can enhance future investigations by linking PET, electroencephalography [90], event-related brain potential (ERP) [91], resting state functional magnetic resonance imaging (rs-fMRI), diffusion tensor imaging (DTI), and movement measurement [92], along with quantitative measurements of FMRP and *fmr1* [3]. Newly developed PET/MRI scanners [81] may produce visualization of the density and distribution of mGluR$_5$s that is superior to images obtained from HRRT co-registered with MRI. PET/MRI units are appealing for future investigations because a single session would be required. PET/MRI provides both functional (PET) and structural (MRI) findings in one encounter. Thus, PET/MRI instrumentation and many other multimodal techniques may be utilized when available for subsequent investigations.

5. Conclusions

We showed the feasibility and safety of applying PET as a tool to quantify mGluR$_5$ receptor expression in the brains of humans with FXS.

We showed that the proposed protocol of MR and PET scans in one day is feasible in individuals with FXS who have received mock scanner training by an experienced behavioral psychology team.

Most importantly, we found for the first time that quantified mGluR$_5$ expression using [^{18}F]FPEB is reduced in the living human brain of men with FXS in contrast to healthy normal age- and sex-matched controls with TD.

Larger studies with additional molecular biomarkers [93] are needed to expand on the feasibility finding of this protocol to evaluate the receptor expression of mGluR$_5$s using [^{18}F]FPEB as a helpful tool for the design of clinical trials of glutamatergic agents in FXS.

Abbreviations

[^{18}F]FPEB	3-[^{18}F]fluoro-5-(2- pyridinylethynyl)benzonitrile
ASD	Autism spectrum disorder
BP$_{ND}$	Non-displaceable binding potential
CDC	Centers for Disease Control and Prevention
DTI	Diffusion tensor imaging
ERK	Extracellular signal-regulated kinase
ERP	Event-related brain potential
FORWARD	Fragile X Online Registry With Accessible Research Database of the National Fragile X Foundation (NFXF)
FMR1	Fragile X mental retardation 1
FMRP	Fragile X Mental Retardation Protein
FXS	Fragile X syndrome
ID	Intellectual disability
LTD	Long-term depression
MAPK	Mitogen-activated protein kinase
MBq	Megabecquerel
mCi	Millicurie
mGluR$_5$	Metabotropic glutamate receptor subtype 5
MRI	Magnetic resonance imaging
mTOR	Mammalian target of rapamycin (mTOR)
NAM	Negative allosteric modulator
NFXF	National Fragile X Foundation
PET	Positron emission tomography
PET/MRI	Positron emission tomography/magnetic resonance imaging
rs-FMRI	Resting-state functional magnetic resonance imaging
RTGA	Reference tissue graphical analysis
SPM	Statistical parametric mapping
TACs	Time activity curves
TD	Typical development
VOIs	Volumes of interest
(period)	Missing data

References

1. Bardoni, B.; Schenck, A.; Mandel, J.-L. The Fragile X Mental Retardation Protein. *Brain Res. Bull.* **2001**, *56*, 375–382. [CrossRef]
2. Brasic, J.R.; Farhadi, F.; Elshourbagy, T. Autism Spectrum Disorder. *Medscape Drugs & Diseases.* Updated 18 March 2020. Available online: http://emedicine.medscape.com/article/912781-overview (accessed on 21 November 2020).

3. Budimirovic, D.B.; Berry-Kravis, E.; Erickson, C.A.; Hall, S.S.; Hessl, D.; Reiss, A.L.; King, M.K.; Abbeduto, L.; Kaufmann, W.E. Updated report on tools to measure outcomes of clinical trials in fragile X syndrome. *J. Neurodev. Disord.* **2017**, *9*, 14. [CrossRef] [PubMed]

4. Budimirovic, D.B.; Kaufmann, W.E. What can we learn about autism from studying fragile X syndrome? *Dev. Neurosci.* **2011**, *33*, 379–394. [CrossRef] [PubMed]

5. Budimirovic, D.B.; Subramanian, M. Neurobiology of autism and intellectual disability: Fragile X syndrome. In *Neurobiology of Disease*, 2nd ed.; Johnston, M.V., Ed.; Oxford University Press: New York, NY, USA, 2016; pp. 375–384.

6. Hagerman, R.J.; Des-Portes, V.; Gasparini, F.; Jacquemont, S.; Gomez-Mantilla, B. Translating molecular advances in fragile X syndrome into therapy: A review. *J. Clin. Psychiatry* **2014**, *75*, e294–e307. [CrossRef] [PubMed]

7. Hagerman, R.J.; Berry-Kravis, E.; Kaufmann, W.E.; Ono, M.Y.; Tartaglia, N.; Lachiewicz, A.; Kronk, R.; Delahunty, C.; Hessl, D.; Visootsak, J.; et al. Advances in the treatment of fragile X syndrome. *Pediatrics* **2009**, *123*, 378–390. [CrossRef] [PubMed]

8. Kaufmann, W.E.; Capone, G.; Clarke, M.; Budimirovic, D.B. Autism in genetic intellectual disability: Insights into idiopathic autism. In *Autism: Current Theories and Evidence*; Zimmerman, A.W., Ed.; The Humana Press Inc.: Totowa, NJ, USA, 2008; pp. 81–108.

9. Pretto, D.I.; Kumar, M.; Cao, Z.; Cunningham, C.L.; Durbin-Johnson, B.; Qi, L.; Berman, R.; Noctor, S.C.; Hagerman, R.J.; Pessah, I.N.; et al. Reduced excitatory amino acid transporter 1 and metabotropic glutamate receptor 5 expression in the cerebellum of fragile X mental retardation gene 1 premutation carriers with fragile X-associated tremor/ataxia syndrome. *Neurobiol. Aging* **2014**, *35*, 1189–1197. [CrossRef]

10. Ascano, M., Jr.; Mukherjee, N.; Bandaru, P.; Miller, J.B.; Nusbaum, J.D.; Corcoran, D.L.; Langlois, C.; Munschauer, M.; Dewell, S.; Hafner, M.; et al. FMRP targets distinct mRNA sequence elements to regulate protein expression. *Nature* **2012**, *492*, 382–386. [CrossRef]

11. Darnell, J.C.; Van Driesche, S.J.; Zhang, C.; Hung, K.Y.S.; Mele, A.; Fraser, C.E.; Stone, E.F.; Chen, C.; Fak, J.J.; Chi, S.W.; et al. FMRP stalls ribosomal translocation on mRNAs linked to synaptic function and autism. *Cell* **2011**, *146*, 247–261. [CrossRef]

12. Budimirovic, D.B.; Schlageter, A.; Filopovic-Sadic, S.; Protic, D.D.; Bram, E.; Mahone, E.M.; Nicholson, K.; Culp, K.; Javanmardi, K.; Kemppainnen, J.; et al. A genotype-phenotype study of high-resolution *FMR1* nucleic acid and protein analyses in fragile X patients with neurobehavioral assessments. *Brain Sci.* **2020**, *10*, 694. [CrossRef]

13. Bagni, C.; Zukin, R.S. A synaptic perspective of fragile X syndrome and autism spectrum disorders. *Neuron* **2019**, *101*, 1070–1088. [CrossRef]

14. Bear, M.F.; Huber, K.M.; Warren, S.T. The mGluR theory of fragile X mental retardation. *Trends Neurosci.* **2004**, *27*, 370–377. [CrossRef] [PubMed]

15. D'Antoni, S.; Spatuzza, M.; Bonaccorso, C.M.; Musumeci, S.A.; Ciranna, L.; Nicoletti, F.; Huber, K.M.; Catania, M.V. Dysregulation of group-1 metabotropic glutamate (mGlu) receptor mediated signalling in disorders associated with intellectual disability and autism. *Neurosci. Biobehav. Rev.* **2014**, *46 (Pt 2)*, 228–241. [CrossRef]

16. Hajós, M. Portraying inhibition of metabotropic glutamate receptor 5 in fragile X mice. *Biol. Psychiatry* **2014**, *75*, 177–178. [CrossRef] [PubMed]

17. Hinton, V.J.; Brown, W.T.; Wisniewski, K.; Rudelli, R.D. Analysis of neocortex in three males with the fragile X syndrome. *Am. J. Med. Genet.* **1991**, *41*, 289–294. [CrossRef] [PubMed]

18. Kaufmann, W.E.; Moser, H.W. Dendritic anomalies in disorders associated with mental retardation. *Cereb. Cortex* **2000**, *10*, 981–991. [CrossRef] [PubMed]

19. Lohith, T.G.; Osterweil, E.K.; Fujita, M.; Jenko, K.J.; Bear, M.F.; Innis, R.B. Is metabotropic glutamate receptor 5 upregulated in prefrontal cortex in fragile X syndrome? *Mol. Autism* **2013**, *4*, 15. [CrossRef]

20. Jong, Y.-J.I.; Harmon, S.K.; O'Malley, K.L. Location and cell-type-specific bias of metabotropic glutamate receptor, mGlu$_5$, negative allosteric modulators. *ACS Chem. Neurosci.* **2019**, *10*, 4558–4570. [CrossRef]

21. DeLorenzo, C.; Gallezot, J.-D.; Gardus, J.; Yang, J.; Planeta, B.; Nabulsi, N.; Ogden, R.T.; Labaree, D.C.; Huang, Y.H.; Mann, J.J.; et al. In vivo variation in same-day estimates of metabotropic glutamate receptor subtype 5 binding using [11C]ABP688 and [18F]FPEB. *J. Cereb. Blood Flow Metab.* **2017**, *37*, 2716–2727. [CrossRef]

22. Ansari, M.S.; Jones, C.K.; Felts, A.S.; Lindsley, C.W.; Alagille, D.; Tamagnan, G.D.; Kessler, R.M.; Baldwin, R.M. One pot synthesis of [18F]FPEB in a semi-automated module. *J. Labelled Comp. Radiopharm.* **2009**, *52* (Suppl. 1), 318.

23. Barret, O.; Tamagnan, G.; Batis, J.; Jennings, D.; Zubal, G.; Russel, D.; Marek, K.; Seibyl, J. Quantitation of glutamate mGluR5 receptor with 18F-FPEB PET in humans. *Neuroimage* **2010**, *52* (Suppl. 1), S202. [CrossRef]

24. Brasic, J.R.; Syed, A.B.; Farhadi, F.; Wong, D.F. PET Scanning in Autism Spectrum Disorder. Medscape Drugs & Diseases. Updated 16 April 2020. Available online: http://emedicine.medscape.com/article/1155568-overview (accessed on 21 November 2020).

25. Fatemi, S.H.; Wong, D.F.; Brašić, J.R.; Kuwabara, H.; Mathur, A.; Folsom, T.D.; Jacob, S.; Realmuto, G.M.; Pardo, J.V.; Lee, S. Metabotropic glutamate receptor 5 tracer [^{18}F]-FPEB displays increased binding potential in postcentral gyrus and cerebellum of male individuals with autism: A pilot PET study. *Cerebellum Ataxias* **2018**, *5*, 3. [CrossRef]

26. Leurquin-Sterk, G.; Postnov, A.; Celen, S.; de Laat, B.; Bormans, G.; Van Laere, K.J. Kinetic modeling and longterm test-retest of 18F-FPEB mGluR5 PET in healthy volunteers. *J. Nucl. Med.* **2015**, *56* (Suppl. 3), 49.

27. Leurquin-Sterk, G.; Postnov, A.; de Laat, B.; Casteels, C.; Celen, S.; Crunelle, C.L.; Bormans, G.; Koole, M.; Van Laere, K. Kinetic modeling and long-term test-retest reproducibililty of the mGluR5 PET tracer 18F-FPEB in human brain. *Synapse* **2016**, *70*, 153–162. [CrossRef] [PubMed]

28. Sullivan, J.M.; Lim, K.; Labaree, D.; Lin, S.-F.; McCarthy, T.J.; Seibyl, J.P.; Tamagnan, G.; Huang, Y.; Carson, R.E.; Ding, Y.-S.; et al. Kinetic analysis of the metabotropic glutamate subtype 5 tracer [18F]FPEB in bolus and bolus plus-constant-infusion studies in humans. *J. Cereb. Blood Flow Metab.* **2013**, *33*, 532–541. [CrossRef] [PubMed]

29. Sullivan, J.; Planeta-Wilson, B.; Lim, K.; Lin, S.F.; Najafzadeh, S.; McCarthy, T.; Ding, Y.S.; Carson, R.E.; Morris, E.D.; Williams, W.A. Test-retest evaluation of [F-18] FPEB, a PET tracer for the mGluR5 receptors in humans. *J. Cereb. Blood Flow Metab.* **2012**, *32* (Suppl. 1), S122–S123.

30. Wong, D.F.; Waterhouse, R.; Kuwabara, H.; Kim, J.; Brašić, J.R.; Chamroonrat, W.; Stabins, M.; Holt, D.P.; Dannals, R.F.; Hamill, T.G.; et al. ^{18}F-FPEB, a PET radiopharmaceutical for quantifying metabotropic glutamate 5 receptors: A first-in-human study of radiochemical safety, biokinetics, and radiation dosimetry. *J. Nucl. Med.* **2013**, *54*, 388–396. [CrossRef]

31. Brašić, J.R.; Mathur, A.K.; Budimirovic, D.B. The urgent need for molecular imaging to confirm target engagement for clinical trials of fragile X syndrome and other subtypes of autism spectrum disorder. *Arch. Neurosci.* **2019**, *6*, e91831. [CrossRef]

32. Innis, R.B.; Cunninghamm, V.J.; Delforge, J.; Fujita, M.; Gjedde, A.; Gunn, R.N.; Holden, J.; Houle, S.; Huang, S.C.; Ichise, M.; et al. Consensus nomenclature for in vivo imaging of reversibly binding radioligands. *J. Cereb. Blood Flow Metab.* **2007**, *27*, 1533–1539. [CrossRef]

33. The Wellcome Centre for Human Neuroimaging, UCL Queen Square Institute of Neurology, London, UK. Statistical Parametric Mapping (SPM). 2020. Available online: http://www.fil.ion.ucl.ac.uk/spm/ (accessed on 21 November 2020).

34. Russell, D.; Jennings, D.; Tamagnan, G.; Seibyl, J.; Koren, A.; Zubal, G.; Marek, K. Evaluation of novel radiotracers targeting non-dopaminergic striatal biomarkers in HD: 18F-FPEB and PET imaging for metabotropic glutamate receptor type 5 (mGluR5) expression in healthy subjects and subjects with Huntington disease (HD). *Neurotherapeutics* **2010**, *7*, 142. [CrossRef]

35. Russell, D.S.; Jennings, D.L.; Tamagnan, G.; Alagilles, D.; Carson, R.E.; Barret, O.; Batis, J.; Koren, A.; Zubal, G.; Seibyl, J.P.; et al. Evaluation of novel radiotracers targeting non-dopaminergic striatal biomarkers in HD: [18F] FPEB and PET imaging for metabotrophic glutamate receptor type 5 (mGluR5) in healthy subjects and subjects with Huntington's disease (HD). *Mov. Disord.* **2010**, *25* (Suppl. 2), S391–S392. [CrossRef]

36. Russell, D.; Tamagnan, G.; Barrett, O.; Seibyl, J.; Marek, K. Evaluation of mGluR5 in early Parkinson's disease using 18F-FPEB PET imaging. *Mov. Disord.* **2010**, *25* (Suppl. 2), S383–S384.

37. Wang, J.Q.; Tueckmantel, W.; Zhu, A.J.; Pellegrino, D.; Brownell, A.L. Synthesis and preliminary biological evaluation of 3-[F-18]fluoro-5-(2-pyridinylethynyl)benzonitrile as a PET radiotracer for imaging metabotropic glutamate receptor subtype 5. *Synapse* **2007**, *61*, 951–961. [CrossRef] [PubMed]

38. Seibyl, J.; Russell, D.; Jennings, D.; Marek, K. Neuroimaging over the course of Parkinson's disease: From early detection of the at-risk patient to improving pharmacotherapy of later-stage disease. *Semin. Nucl. Med.* **2012**, *42*, 406–414. [CrossRef] [PubMed]

39. Berry-Kravis, E.; Des Portes, V.; Hagerman, R.; Jacquemont, S.; Charles, P.; Visootsak, J.; Brinkman, M.; Rerat, K.; Koumaras, B.; Zhu, L.; et al. Mavoglurant in fragile X syndrome: Results of two randomized, double-blind, placebo-controlled trials. *Sci. Transl. Med.* **2016**, *8*, 321ra5. [CrossRef]

40. Berry-Kravis, E.; Hagerman, R.; Visootsak, J.; Budimirovic, D.; Kaufmann, W.E.; Cherubini, M.; Zarevics, P.; Walton-Bowen, K.; Wang, P.; Bear, M.F.; et al. Arbaclofen in fragile X syndrome: Results of phase 3 trials. *J. Neurodev. Disord.* **2017**, *9*, 3. [CrossRef]

41. Berry-Kravis, E.; Hessl, D.; Coffey, S.; Hervey, C.; Schneider, A.; Yuhas, J.; Hutchison, J.; Snape, M.; Tranfaglia, M.; Nguyen, D.V.; et al. A pilot open label, single dose trial of fenobam in adults with fragile X syndrome. *J. Med. Genet.* **2009**, *46*, 266–271. [CrossRef]

42. Berry-Kravis, E.M.; Hessl, D.; Rathmell, B.; Zarevics, P.; Cherubini, M.; Walton-Bowen, K.; Mu, Y.; Nguyen, D.V.; Gonzalez-Heydrich, J.; Wang, P.P.; et al. Effects of STX209 (arbaclofen) on neurobehavioral function in children and adults with fragile X syndrome: A randomized, controlled, phase 2 trial. *Sci. Transl. Med.* **2012**, *4*, 152ra127. [CrossRef]

43. Berry-Kravis, E.; Hessl, D.; Abbeduto, L.; Reiss, A.L.; Beckel-Mitchener, A.; Urv, T.K. Outcome measures for clinical trials in fragile X syndrome. *J. Dev. Behav. Pediatr.* **2013**, *34*, 508–522. [CrossRef]

44. Berry-Kravis, E.M.; Lindemann, L.; Jønch, A.E.; Apostol, G.; Bear, M.F.; Carpenter, R.L.; Crawley, J.N.; Curie, A.; Des Portes, V.; Hossain, F.; et al. Drug development for neurodevelopmental disorders: Lessons learned from fragile X syndrome. *Nat. Rev. Drug Discov.* **2018**, *17*, 280–299. [CrossRef]

45. Budimirovic, D.B.; Duy, P.Q. Neurobehavioral features and targeted treatments in fragile X syndrome: Current insights and future directions. *Engrami* **2015**, *37*, 5–19. [CrossRef]

46. Budimirovic, D.B.; Duy, P.Q. Challenges in translating therapeutic frontiers in clinical trials: Where are we now and what's next? *Madridge J. Neuroscience* **2016**, *1*, e1–e3. [CrossRef]

47. Duy, P.Q.; Budimirovic, D.B. Fragile X syndrome: Lessons learned from the most translated neurodevelopmental disorder in clinical trials. *Transl. Neurosci.* **2017**, *8*, 7–8. [CrossRef] [PubMed]

48. Erickson, C.A.; Davenport, M.H.; Schaefer, T.L.; Wink, L.K.; Pedapati, E.V.; Sweeney, J.A.; Fitzpatrick, S.E.; Brown, W.T.; Budimirovic, D.; Hagerman, R.J.; et al. Fragile X targeted pharmacotherapy: Lessons learned and future directions. *J. Neurodev. Disord.* **2017**, *9*, 7. [CrossRef] [PubMed]

49. Jønch, A.E.; Jacquemont, S. Reflections on clinical trials in fragile X syndrome. In *Fragile X Syndrome: From Genetics to Targeted Treatment*; Willemsen, R., Kooy, R.F., Eds.; Academic: London, UK, 2017; pp. 419–441.

50. Ligsay, A.; Hagerman, R.; Berry-Kravis, E. Overview of targeted double-blind, placebo-controlled clinical trials in fragile X syndrome. In *Fragile X Syndrome: From Genetics To Targeted Treatment*; Willemsen, R., Kooy, R.F., Eds.; Academic: London, UK, 2017; pp. 401–418.

51. Ligsay, A.; Van Dijck, A.; Nguyen, D.V.; Lozano, R.; Chen, Y.; Bickel, E.S.; Hessl, D.; Schneider, A.; Angkustsir, K.; Tassone, F.; et al. A randomized double-blind, placebo controlled trial of ganaxolone in children and adolescents with fragile X syndrome. *J. Neurodev. Disord.* **2017**, *9*, 26. [CrossRef]

52. Russell, D. A PET Brain Imaging Study of mGluR5 in Subjects with Neuropsychiatric Conditions (FPEB). ClinicalTrials.gov Identifier: NCT00870974 2017. Available online: https://clinicaltrials.gov/ct2/show/NCT00870974 (accessed on 21 November 2020).

53. World Medical Association. Declaration of Helsinki: Medical Research Involving Human Subjects. 2013. Available online: https://www.wma.net/what-we-do/medical-ethics/declaration-of-helsinki/ (accessed on 21 November 2020).

54. International Committee of Medical Journal Editors (ICMJE). Recommendations for the Conduct, Reporting, Editing, and Publication of Scholarly Work in Medical Journals. 2019. Available online: http://www.icmje.org/icmje-recommendations.pdf (accessed on 21 November 2020).

55. Brasic, J.R.; Nandi, A.; Russell, D.S.; Jennings, D.; Barret, O.; Mathur, A.; Slifer, K.; Sedlak, T.; Martin, S.D.; Brinson, Z.; et al. Dataset of Reduced cerebral expression of metabotropic glutamate receptor subtype 5 in men with fragile X syndrome. Available online: https://doi.org/10.5281/zenodo.4279744 (accessed on 23 November 2020).

56. Deb, S.; Hare, M.; Prior, L.; Bhaumick, S. Dementia Screening Questionnaire for Individuals with Intellectual Disabilities. *Br. J. Psychiatry* **2007**, *190*, 440–444. [CrossRef]

57. Roid, G.H. *Stanford-Binet Intelligence Scales*, 5th ed.; (SB-5); Western Psychological Services (WPS): Torrance, CA, USA, 2003.

58. Hessl, D.; Nguyen, D.V.; Green, C.; Chavez, A.; Tassone, F.; Hagerman, R.J.; Senturk, D.; Schneider, A.; Lightbody, A.; Reiss, A.L.; et al. A solution to limitations of cognitive testing in children with intellectual disabilities: The case of fragile X syndrome. *J. Neurodev. Disord.* **2009**, *1*, 33–45. [CrossRef]

59. Sparrow, S.S.; Cicchetti, D.V.; Saulnier, C.A. *Vineland Adaptive Behavior Scales*, 3rd ed.; (Vineland-3); Pearson: San Antonio, TX, USA, 2020.

60. Brašić, J.R.; Zhou, Y.; Musachio, J.L.; Hilton, J.; Fan, H.; Crabb, A.; Endres, C.J.; Reinhardt, M.J.; Dogan, A.S.; Alexander, M.; et al. Single photon emission computed tomography experience with (*S*)5-[^{123}I]iodo-3-(2-azetidinylmethoxy)pyridine in the living human brain of smokers and nonsmokers. *Synapse* **2009**, *63*, 339–358. [CrossRef]

61. Wienhard, K.; Dahlbom, M.; Eriksson, L.; Michel, C.; Bruckbauer, T.; Pietrzyk, U.; Heiss, W.-D. The ECAT EXACT HR: Performance of a new high resolution positron scanner. *J. Comput. Assist. Tomogr.* **1994**, *18*, 110–118. [CrossRef]

62. Cox, A.D.; Virues-Ortega, J.; Julio, F.; Martin, T.L. Establishing motion control in children with autism and intellectual disability: Applications for anatomical and functional MRI. *J. Appl. Behav. Anal.* **2017**, *50*, 8–26. [CrossRef]

63. Slifer, K.J.; Cataldo, M.F.; Cataldo, M.D.; Llorente, A.M.; Gerson, A.C. Behavior analysis of motion control for pediatric neuroimaging. *J. Appl. Behav. Anal.* **1993**, *26*, 469–470. [CrossRef]

64. Slifer, K.J.; Koontz, K.L.; Cataldo, F. Operant-contingency-based preparation of children for functional magnetic resonance imaging. *J. Appl. Behav. Anal.* **2002**, *35*, 191–194. [CrossRef] [PubMed]

65. Brašić, J.R.; Bibat, G.; Kumar, A.; Zhou, Y.; Hilton, J.; Yablonski, M.E.; Dogan, A.S.; Guevara, M.R.; Stephane, M.; Johnston, M.; et al. Correlation of the vesicular acetylcholine transporter densities in the striata to the clinical abilities of women with Rett syndrome. *Synapse* **2012**, *66*, 471–482. [CrossRef] [PubMed]

66. Brašić, J.R.; Cascella, N.; Kumar, A.; Zhou, Y.; Hilton, J.; Raymont, V.; Crabb, A.; Guevara, M.R.; Horti, A.G.; Wong, D.F. Positron emission tomography (PET) experience with 2-[18F]fluoro-3-(2(S)-azetidinylmethoxy) pyridine (2-[18F]FA) in the living human brain of smokers with paranoid schizophrenia. *Synapse* **2012**, *66*, 352–368. [CrossRef] [PubMed]

67. Rahmim, A.; Cheng, J.-C.; Blinder, S.; Camborde, M.-L.; Sossi, V. Statistical dynamic image reconstruction in state-of-the-art high-resolution PET. *Phys. Med. Biol.* **2005**, *50*, 4887–4912. [CrossRef] [PubMed]

68. Sossi, V.; de Jong, H.W.A.M.; Barker, W.C.; Bloomfield, P.; Burbar, Z.; Camborde, M.-L.; Comtat, C.; Eriksson, L.A.; Houle, S.; Keator, D.; et al. The second generation HRRT—A multi-centre scanner performance investigation. *IEEE Nucl. Sci. Symp. Conf. Ref.* **2005**, *4*, 2195–2199.

69. Fischl, B.; van der Kouwe, A.; Destrieux, C.; Halgren, E.; Ségonne, F.; Salat, D.H.; Busa, E.; Seidman, L.J.; Goldstein, J.; Kennedy, D.; et al. Automatically parcellating the human cerebral cortex. *Cereb. Cortex* **2004**, *14*, 11–22. [CrossRef]

70. Hoopes, A. (Ed.) FreeSurfer Download and Install. 2020. Available online: https://surfer.nmr.mgh.harvard.edu/fswiki/DownloadAndInstall (accessed on 21 November 2020).

71. Jenkinson, M.; Beckmann, C.F.; Behrens, T.E.J.; Woolrich, M.W.; Smith, S.M. FSL. *Neuroimage* **2012**, *62*, 782–790. [CrossRef]

72. Patenaude, B.; Smith, S.M.; Kennedy, D.N.; Jenkinson, M. A Bayesian model of shape and appearance for subcortical brain segmentation. *Neuroimage* **2011**, *56*, 907–922. [CrossRef]

73. Woolrich, M.W.; Jbabdi, S.; Patenaude, B.; Chappell, M.; Makni, S.; Behrens, T.; Beckmann, C.; Jenkinson, M.; Smith, S.M. Bayesian analysis of neuroimaging data in FSL. *Neuroimage* **2009**, *45* (Suppl. 1), S173–S186. [CrossRef] [PubMed]

74. Ashburner, J.; Friston, K.J. High-dimensional image warping. In *Human Brain Function*, 2nd ed.; Frackowiak, R.S.J., Ashburner, J., Penny, W.D., Zeki, S., Friston, K.J., Frith, C., Dolan, R., Price, C.J., Eds.; Academic: Waltham, MA, USA, 2004; pp. 656–673.

75. Ashburner, J.; Friston, K.J. Rigid body registration. In *Human Brain Function*, 2nd ed.; Frackowiak, R.S.J., Ashburner, J., Penny, W.D., Zeki, S., Friston, K.J., Frith, C., Dolan, R., Price, C.J., Eds.; Academic: Waltham, MA, USA, 2004; pp. 635–654.

76. Logan, J.; Volkow, N.D.; Wang, G.J.; Ding, Y.S.; Alexoff, D.L. Distribution volume ratios without blood sampling from graphical analysis of PET data. *J. Cerebral. Blood Flow Metab.* **1996**, *16*, 834–840. [CrossRef]

77. Logan, J.; Alexoff, D.; Fowler, J.S. The use of alternative forms of graphical analysis to balance bias and precision in PET images. *J. Cereb. Blood Flow Metab.* **2011**, *31*, 535–546. [CrossRef]

78. Carson, R.E. Tracer kinetic modeling in PET. In *Positron Emission Tomography: Basic Science and Clinical Practice*; Valk, P.E., Bailey, D.L., Townsend, D.W., Maisey, M.N., Eds.; Springer: London, UK, 2003; pp. 147–179.

79. Wickham, H. *ggplot2: Elegant Graphics for Data Analysis*; Springer: New York, NY, USA, 2009.

80. R Core Team. *R: A Language and Environment for Statistical Computing*; R Foundation for Statistical Computing: Vienna, Austria, 2017; Available online: https:www.R-project-org (accessed on 29 September 2020).

81. Catana, C. Principles of simultaneous PET/MR imaging. *Magn. Reson. Imaging Clin. N. Am.* **2017**, *25*, 231–243. [CrossRef]

82. Trivedi, R.R.; Bhattacharyya, S. Constitutive internalization and recycling of metabotropic glutamate receptor 5 (mGluR5). *Biochem. Biophys. Res. Commun.* **2012**, *427*, 185–190. [CrossRef]

83. Castañeda, T.R.; de Prado, B.M.; Prieto, D.; Mora, F. Circadian rhythms of dopamine, glutamate and GABA in the striatum and nucleus accumbens of the awake rat: Modulation by light. *J. Pineal Res.* **2004**, *36*, 177–185. [CrossRef] [PubMed]

84. Fuller, P.M.; Gooley, J.J.; Saper, C.B. Neurobiology of the sleep-wake cycle: Sleep architecture, circadian regulation, and regulatory feedback. *J. Biol. Rhythm.* **2006**, *21*, 482–493. [CrossRef] [PubMed]

85. Meng, T.; Yuan, S.; Zheng, Z.; Liu, T.; Lin, L. Effects of endogenous melatonin on glutatmate and GABA rhythms in the striatum of unilateral 6-hydroxydopamine-lesioned rats. *Neuroscience* **2015**, *286*, 308–315. [CrossRef] [PubMed]

86. Brasic, J.; Budimirovic, D.; Mathur, A.; Nandi, A.; Mahone, E.; Slifer, K.; Brinson, Z.; Sedlak, T.; Ryan, M.; Landa, R.; et al. Metabotropic Glutamate Receptor Subtype 5 Function in Fragile X Syndrome. *J. Nucl. Med.* **2020**, *61* (Suppl. 1), 1552. Available online: http://jnm.snmjournals.org/content/61/supplement_1/1552.abstract?sid=7a58a0b9-ec27-42f3-b06e-7ded1f2dc2c8 (accessed on 21 November 2020).

87. Darnell, R.B. The genetic control of stoichiometry underlying autism. *Annu. Rev. Neurosci.* **2020**, *43*, 509–533. [CrossRef] [PubMed]

88. Jacquemont, S.; Pacini, L.; Jønch, A.E.; Cencelli, G.; Rozenberg, I.; He, Y.; D'Andrea, L.; Pedini, G.; Eldeeb, M.; Willemsen, R.; et al. Protein synthesis levels are increased in a subset of individuals with fragile X syndrome. *Hum. Mol. Genet.* **2018**, *27*, 2039–2051, Erratum in: *Hum. Mol. Genet.* **2018**, *27*. [CrossRef]

89. Schmidt, K.C.; Loutaev, I.; Quezado, Z.; Sheeler, C.; Smith, C.B. Regional rates of brain protein synthesis are unaltered in dexmedetomidine sedated young men with fragile X syndrome: A L-[1-^{11}C]leucine PET study. *Neurobiol. Dis.* **2020**, *143*, 104978. [CrossRef]

90. Razak, K.A.; Dominick, K.C.; Erickson, C.A. Developmental studies in fragile X syndrome. *J. Neurodev. Disord.* **2020**, *12*, 13. [CrossRef]

91. Li, W.; Kutas, M.; Gray, J.A.; Hagerman, R.H.; Olichney, J.M. The role of glutamate in language and language disorders—Evidence from ERP and pharmacological studies. *Neurosci. Biobehav. Rev.* **2020**, *119*, 217–241. [CrossRef] [PubMed]

92. McKay, G.N.; Harrigan, T.P.; Brasic, J.R. A low-cost quantitative continuous measurement of movements in the extremities of people with Parkinson's disease. *MethodsX* **2019**, *6*, 169–189. [CrossRef] [PubMed]

93. Zafarullah, M.; Tassone, F. Molecular biomarkers in fragile X syndrome. *Brain Sci.* **2019**, *9*, 96. [CrossRef] [PubMed]